International Conference on Applied Energy 2020
Dec. 1 - Dec. 10, 2020, Bangkok / Virtual
Paper ID: 293

A Detailed Distributed Parameter Model for Accurate Performance Assessment of Power-to-Methane System

Like Zhong, Erren Yao, Hansen Zou, Guang Xi*

School of Energy and Power Engineering, Xi'an Jiaotong University, Xi'an 710049, Shaanxi, China

ABSTRACT

Power-to-methane based on the solid oxide electrolysis cell is considered as a promising technology for energy storage. Most research employed the lumped parameter method to establish the core components' model (i.e., solid oxide electrolysis cell and/or methanation reactor) for the performance analysis of the overall power-to-methane system, which is unable to reveal the performance of the core components accurately. Thereby the safety and stability of the overall system cannot be evaluated reasonably. In this paper, the distributed parameter method for the model of the core components is conducted to evaluate the performance of the overall system reasonably with the consideration of the temperature gradient of the solid oxide electrolysis cell as well as the maximum temperature of the methanation reactor. The results indicate that the temperature gradient of the solid oxide electrolysis cell should be kept as low as possible with the increasing overall efficiency and methane yield, and it is necessary to control the operating temperature of the methanation reactor in a rational range to avoid the non-ignition and catalyst deactivation.

Keywords: energy storage, power-to-methane, solid oxide electrolysis cell, methanation reactor, distributed parameter method, performance assessment.

NOMENCLATURE

Abbreviations	
MM	membrane module
MR	methanation reactor
SNG	synthetic natural gas
SOEC	solid oxide electrolysis cell
PtM	power to methane
Symbols	
n	molar flow rate
P	pressure
TC	temperature
TG	temperature gradient
V_{op}	voltage
W	power
η	efficiency

1. INTRODUCTION

Energy storage has become a vital issue to address the mismatching between energy consumption and supply due to the random and intermittent nature of renewable energy. Among available energy storage technologies (i.e., pumped-hydro, compressed-air, batteries, and power-to-gas), power-to-methane (PtM) technology has drawn more and more attention worldwide due to its advantages of flexibility, high energy density, large-scale infrastructure, and long-timescale storage [1]. The two core components of PtM are the electrolyzer and the methanation reactor (MR). The electrolyzer can split water into H_2 and O_2 by the surplus electrical power, and then H_2 further reacts with CO_2 in the MR for the production of the synthetic natural gas (SNG). Available electrolysis technologies mainly include low-temperature Alkaline Electrolysis Cell (AEC) and Proton Exchange Membrane Electrolysis Cell (PEMEC), and high-temperature Solid Oxide Electrolysis Cell (SOEC) [2]. Compared with the AEC and PEMEC, SOEC can obtain a high electrolysis efficiency with much lower cell voltage and moderate current density, and the integration between the SOEC and strongly exothermic methanation process can achieve a high overall efficiency of the PtM system [3].

Some scholars investigated the design and optimization of the SOEC-based PtM from the level of the overall system to improve the overall efficiency and SNG yield. However, most of these studies employed the lumped parameter method for the analysis of the

Selection and peer-review under responsibility of the scientific committee of the 12th Int. Conf. on Applied Energy (ICAE2020).

SOEC [4-6] or MR [7-9], which is unable to present some crucial parameter profiles (e.g. temperature and concentration) of the SOEC and MR. Therefore, the high thermal stress and excessive concentration consumption in the SOEC cannot be revealed as well as the catalyst deactivation and thermal runaway in the MR. Furthermore, the safe and stable operation of the overall system cannot be evaluated.

To solve the above problems, this paper establishes an accurate thermodynamic model to reasonably assess the performance of the SOEC-based PtM system with the distributed parameter method for the SOEC and MR. Detailed system description and mathematical model are presented in sections 2 and 3, respectively. Besides, the effects of some key parameters on the system performance are investigated to understand the characteristics of the core components and overall system.

2. SYSTEM DESCRIPTION

The configuration of the PtM system is illustrated in Fig. 1. It mainly consists of the SOEC, MR, and MM. The water is pumped firstly into the system and preheated by the mixed gas leaving from the FPH, and then is split into two streams. One stream recovers the heat of the exothermic methanation process for the steam generation, and another is heated to the steam by the exhausted air. Next, the two streams merge and then mix with a part of fuel gas produced by the SOEC to maintain 10 vol.% of H_2. After that, the reactant feed is further heated in the FR and FEH in sequence before delivery to the SOEC. At the same time, the air is supplied into the system and then is heated in the APH, AR, and AEH in turn before entering into the SOEC. In the SOEC, the H_2-rich fuel gas and O_2-rich air are produced by the electrochemical reaction. Next, the exhausted air flows through the AR and SG and expands in the AT to generate power. On the other hand, a part of fuel gas is circulated to the MIX1, and another part of fuel gas is cooled for the unreacted water separation. The dry H_2 mixes with CO_2 and the permeate from the MM, and then the mixed gas is heated before flowing into the MR for the SNG production. The outgoing gas of the MR is cooled with the condensed water knocked out. Finally, the dry gas mixture is compressed and enters into the MM to obtain high-purity methane.

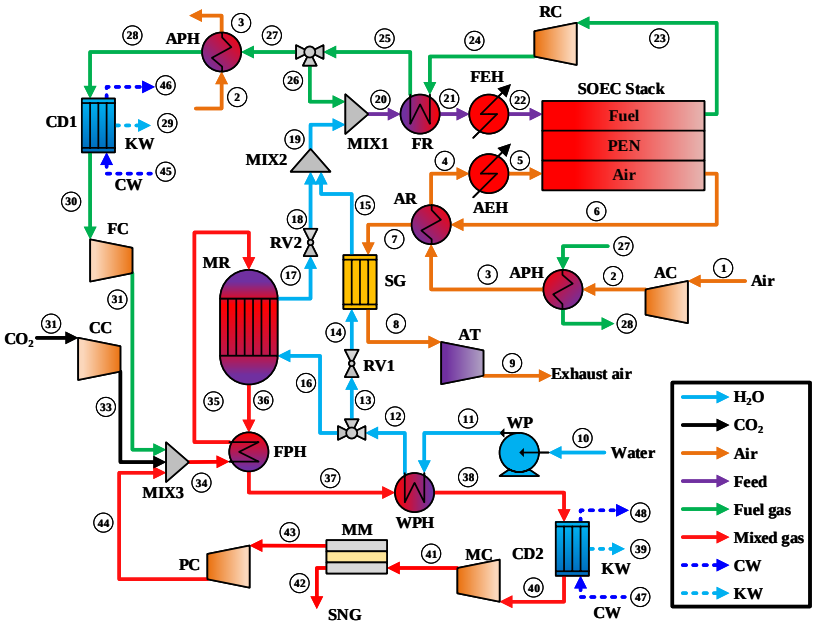

Fig. 1 The configuration of the PtM system. SOEC: solid oxide electrolysis cell; MR: methanation reactor; MM: membrane module; AT: air turbine; WP: water pump; AC: air compressor; CC: CO_2 compressor; FC: fuel compressor; PC: permeate compressor; RC: recycle compressor; MC: methane compressor; AEH: air electrical heater; FEH: feed electrical heater; APH: air preheater; FPH: fuel preheater; WPH: water preheater; AR: air regenerator; FR: feed regenerator; SG: steam generator; CD: condenser; RV: relief valve; CW: cooling water; KW: knockout water.

3. THERMODYNAMIC MODEL

3.1 Solid oxide electrolysis cell

The 1D model for the SOEC stack is developed with the equations adapted from Refs. [9-12]. The electrochemical reaction is described by the voltage,

current density, temperature, pressure, and species concentration. The temperature gradient along the direction of the gas flow, which is a vital indicator of the thermal stress of the SOEC, can be presented by the 1D model. The larger thermal stress caused by a higher temperature gradient can induce the fracture of the SOEC [13], and further lead to the breakdown of the overall system. Therefore, the maximum temperature gradient of the SOEC should be kept as low as possible.

3.2 Methanation reactor

In the MR, the exothermic Sabatier reaction (Eq. (3)) accompanied by reverse water gas shift (Eq. (2)) and CO methanation (Eq. (1)) occurs as follows:

$$CO + 3H_2 \leftrightarrow CH_4 + H_2O \quad \Delta H = -206.1\ \text{kJ/mol} \quad (1)$$

$$CO + H_2 \leftrightarrow CO + H_2O \quad \Delta H = +41.2\ \text{kJ/mol} \quad (2)$$

$$CO_2 + 4H_2 \leftrightarrow CH_4 + 2H_2O \quad \Delta H = -164.9\ \text{kJ/mol} \quad (3)$$

The 1D pseudo-homogeneous plug-flow reactor model is implemented to describe the methanation process [14]. The kinetic equations proposed by Xu and Froment [15] are employed to determine the reaction rates. The temperature profile of the MR is controlled by the catalyst loading, the number of the reaction tube, and cooling water, and the allowable maximum temperature is determined as 700 °C [16] to avoid the catalyst sintering. The heat transfer between the reactant gas and cooling water is modeled according to the thermal conductivity model proposed by Tsotsas[17], Martin and Nilles [18].

3.3 Balance of plant

The MM is modeled by the 1D model with consideration of the different gas permeability [19]. The 1D counter-flow model is applied to the heat exchangers (HEX), and the heat transfer models of single-phase and two-phase flow are calculated respectively according to the Refs. [20-22]. Besides, the multi-stage adiabatic compressors with the inter-stage cooling are employed. All stage compressors have the same pressure ratio and the same isentropic efficiency of 75%. Moreover, the isentropic efficiency of 80% for AT is considered.

4. RESULTS AND DISCUSSION

The effects of some key parameters on the overall efficiency and SNG yield of the PtM system are investigated, and the temperature profiles of the SOEC and MR are considered simultaneously to ensure the safety of the overall system. The input parameters and simulation results under the design condition are listed in Table 1. The temperature gradient of the SOEC and the temperature distribution of the MR are presented in Fig. 2. The negative value of the SOEC temperature gradient means the SOEC operates under the endothermic condition, and the temperature gradient is gradually decreased because of the reduced electrochemical reaction along the direction of the gas flow. The temperature of the MR increases rapidly first due to the strongly exothermic methanation reaction and then has a drop under the cooling effect of water. The maximum temperature of 651.83 °C is presented.

Table 1. Input parameters and simulation results of the PtM system.

	Parameters	Values
Input	Flow rate of water (mol/s), n_{H2O}	3.0
	Air feed ratio, *AFR*	2
	Inlet temperature of SOEC (°C), $TC_{SOEC,in}$	800
	Inlet pressure of SOEC (kPa), $P_{SOEC,in}$	111.46
	Operating voltage of SOEC (V), V_{SOEC}	1.25
	Inlet temperature of MR (°C), $TC_{MR,in}$	260
	Inlet pressure of MR (kPa), $P_{MR,in}$	1013.3
	Cooling temperature of MR (°C), $TC_{MR,cool}$	250
	HEX pinch point temperature (°C), TC_{pinch}	40
Output	HHV efficiency of system(%), η_{PtM}	79.65
	Exergy efficiency of system(%), $\eta_{Ex,tot}$	75.16
	SNG yield (mol/s), n_{SNG}	0.6174
	Current density of SOEC (A/cm^2), *J*	0.5866
	Feed utilization factor of SOEC, U_f	0.79
	Maximum temperature gradient of SOEC (°C/mm), $TG_{max,SOEC}$	-3.03
	Maximum temperature of MR (°C) $TC_{max,MR}$	651.83

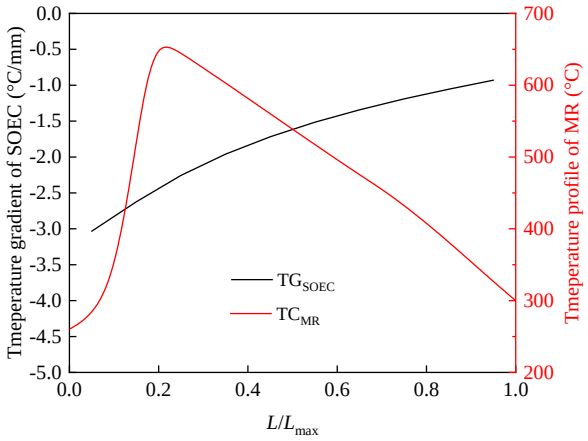

Fig. 2 The temperature gradient of the SOEC and the temperature profile of the MR.

4.1 Effects of water flow rate on the system performance

The effects of water flow rate (n_{H2O}) on the system performance are illustrated in Fig. 3. More water supplied to the system elevates the PtM power consumption (W_{PtM}) as well as the SNG yield (n_{SNG}). It is mainly due to the increment of the SOEC power and H_2 improved by the raised current density. Meanwhile, the decrement of the total efficiency (η_{PtM}) reveals that the increment rate of the consumed power outweighs that of the SNG yield. Because more reaction heat of the MR is taken away by the raised water and then supplied to the SOEC, both the maximum temperature gradient of the SOEC ($TG_{max,SOEC}$) and the maximum temperature of the MR ($TC_{max,MR}$) are reduced.

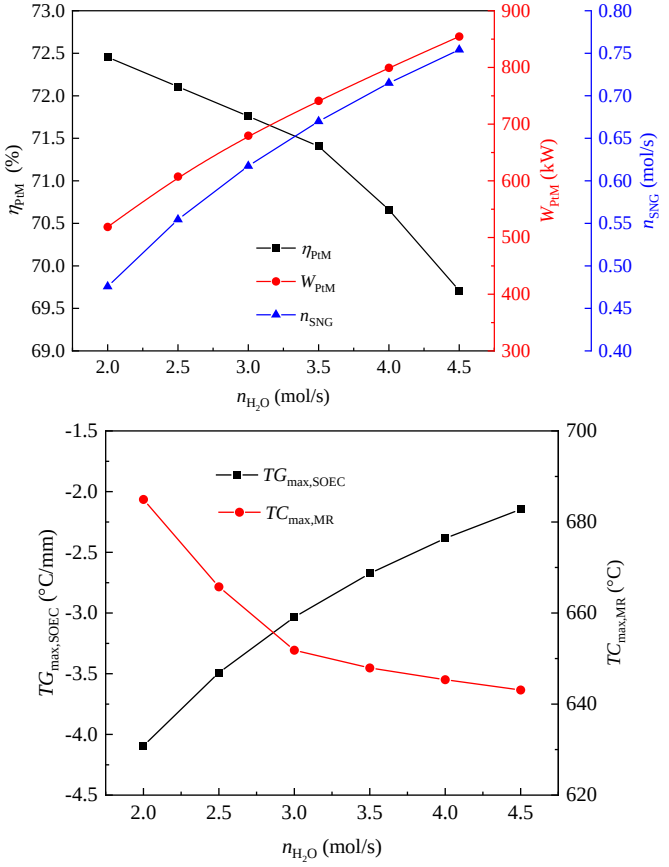

Fig. 3 Effects of water flow rate on the system performance.

4.2 Effects of SOEC voltage on the system performance

The effects of the SOEC voltage (V_{SOEC}) on the system performance are presented in Fig. 4. The current density is improved by the elevated voltage, thereby leading to the higher W_{PtM} and SNG yield. The increment rate of the SNG yield outperforms that of W_{PtM}, leading to an increased η_{PtM}. Meanwhile, more heat is generated by the raised polarization loss of the SOEC, which reduces the $TG_{max,SOEC}$. The $TC_{max,MR}$ firstly declines to a minimum value and then rises rapidly, this is because the reaction heat is less initially and more after that compared with the recovered heat by the cooling water.

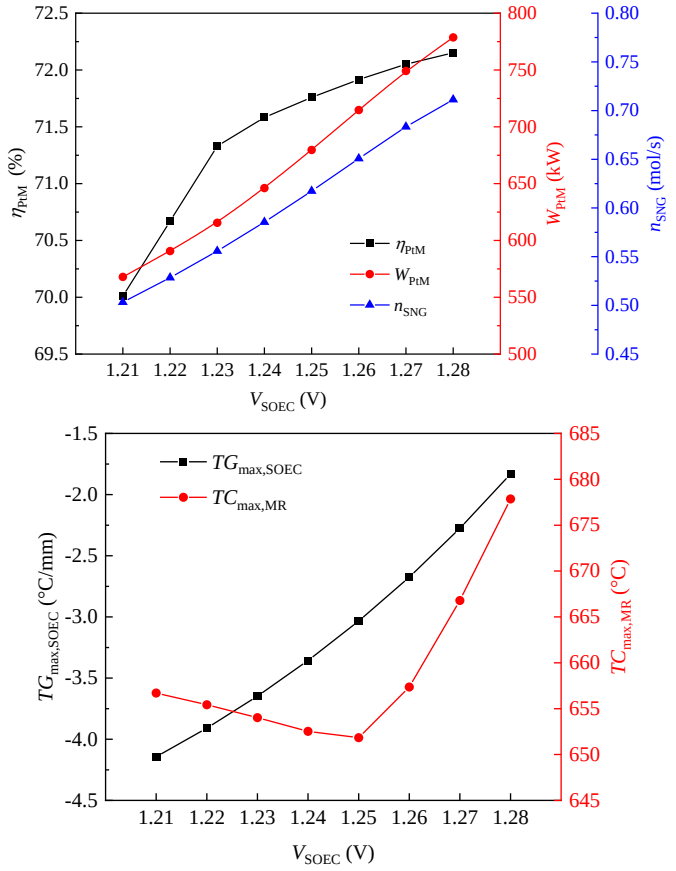

Fig. 4 Effects of SOEC voltage on the system performance.

4.3 Effects of SOEC operating pressure on the system performance

The effects of the SOEC operating pressure (P_{SOEC}) on the system performance are showed in Fig. 5. Under the pressurized condition, the current density is reduced, thereby both SOEC power and SNG yield have declined trendies. Moreover, the elevated pressure also improves the AC and AT power but reduced the FC power. As a result, the decrement rate of W_{PtM} is higher at the beginning and then lower compared with that of the SNG yield, leading to a maximum value of η_{PtM} at the SOEC pressure of 2 bar. The reduced current density reveals that less heat is consumed for the steam split, meaning the smaller $TG_{max,SOEC}$. Besides, with the influence of the heat transfer, the $TC_{max,MR}$ achieves an increasing trend.

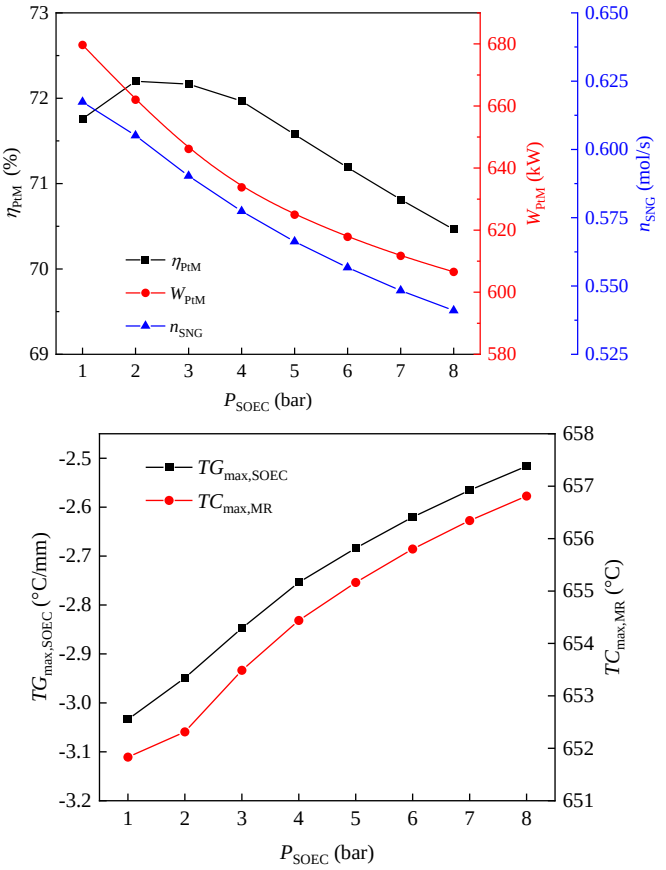

Fig 5 Effects of SOEC operating pressure on the system performance.

4.4 Effects of MR inlet temperature on the system performance

The effects of the MR inlet temperature ($TC_{MR,in}$) on the system performance are illustrated in Fig. 6. It is expected that the $TC_{max,MR}$ has an increment with a higher inlet temperature. Because the low temperature is favorable for methane production, the improved reaction temperature reduces the SNG concentration at the outlet of the MR. As a result, more H_2 is recycled back to the MR inlet at the cost of more power consumption of the MC and PC, which leads to a reduced η_{PtM}. However, it is noted that the lower inlet temperature should be limited because the MR will be in a non-ignited state at the inlet temperature below the limitation (i.e., 260 °C in the present work).

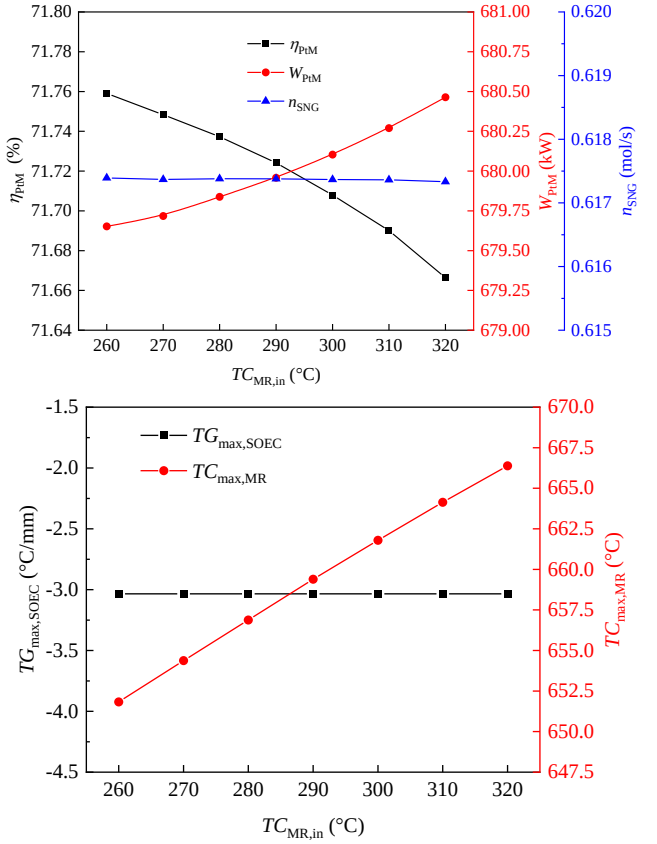

Fig 6 Effects of MR inlet temperature on the system performance.

5. CONCLUSIONS

The distributed parameter method is implemented to model the SOEC and MR for the accurate performance analysis of the overall power-to-methane system. The overall efficiency and SNG yield of the system as well as the temperature profiles of the SOEC and MR are employed as indicators to reasonably assess the system. The increased water flow rate can improve the SNG yield but reduce the overall efficiency, and the SOEC voltage has a positive effect on the system performance. Moreover, the SNG yield is declined by the higher SOEC operating pressure, while the maximum overall efficiency is obtained at the pressure of 2.0 bar. Besides, the PtM efficiency is decreased with a higher MR inlet temperature due to the lower H_2 conversion efficiency. The temperature gradient of the SOEC should be kept as low as possible for the reduction of the failure risk caused by the thermal stress, and the temperature of the MR should be controlled in a rational range to keep the MR in an ignited state and avoid the catalyst deactivation.

ACKNOWLEDGEMENT

The study is supported by China Postdoctoral Science Foundation (Grant No. 2020M683477).

REFERENCE

[1] Thema M, Bauer F, Sterner M. Power-to-Gas: Electrolysis and methanation status review. Renewable and Sustainable Energy Reviews. 2019;112:775-87.

[2] Xing X, Lin J, Song Y, Zhou Y, Mu S, Hu Q. Modeling and operation of the power-to-gas system for renewables integration: a review. CSEE J Power Energy. 2018;4:168-78.

[3] Wang L, Pérez-Fortes M, Madi H, Diethelm S, herle JV, Maréchal F. Optimal design of solid-oxide electrolyzer based power-to-methane systems: A comprehensive comparison between steam electrolysis and co-electrolysis. Appl Enrg. 2018;211:1060-79.

[4] Fujiwara N, Tada S, Kikuchi R. Power-to-gas systems utilizing methanation reaction in solid oxide electrolysis cell cathodes: a model-based study. Sustainable Energy & Fuels. 2020.

[5] Giglio E, Lanzini A, Santarelli M, Leone P. Synthetic natural gas via integrated high-temperature electrolysis and methanation: Part I—Energy performance. Journal of Energy Storage. 2015;1:22-37.

[6] Cao Y, parikhani T. A solar-driven lumped SOFC/SOEC system for electricity and hydrogen production: 3E analyses and a comparison of different multi-objective optimization algorithms. J Clean Prod. 2020;271:122457.

[7] Reznicek EP, Braun RJ. Reversible solid oxide cell systems for integration with natural gas pipeline and carbon capture infrastructure for grid energy management. Appl Enrg. 2020;259:114118.

[8] Salomone F, Giglio E, Ferrero D, Santarelli M, Pirone R, Bensaid S. Techno-economic modelling of a Power-to-Gas system based on SOEC electrolysis and CO_2 methanation in a RES-based electric grid. Chem Eng J. 2019;377:120233.

[9] Wang L, Rao M, Diethelm S, Lin T-E, Zhang H, Hagen A, et al. Power-to-methane via co-electrolysis of H_2O and CO_2: The effects of pressurized operation and internal methanation. Appl Enrg. 2019;250:1432-45.

[10] Menon V, Fu Q, Janardhanan VM, Deutschmann O. A model-based understanding of solid-oxide electrolysis cells (SOECs) for syngas production by H_2O/CO_2 co-electrolysis. J Power Sources. 2015;274:768-81.

[11] Suwanwarangkul R, Croiset E, Fowler MW, Douglas PL, Entchev E, Douglas MA. Performance comparison of Fick's, dusty-gas and Stefan–Maxwell models to predict the concentration overpotential of a SOFC anode. J Power Sources. 2003;122:9-18.

[12] Kazempoor P, Braun RJ. Model validation and performance analysis of regenerative solid oxide cells: Electrolytic operation. Int J Hydrogen Energ. 2014;39:2669-84.

[13] Aguiar P, Adjiman CS, Brandon NP. Anode-supported intermediate temperature direct internal reforming solid oxide fuel cell. I: model-based steady-state performance. J Power Sources. 2004;138:120-36.

[14] Kiewidt L, Thöming J. Predicting optimal temperature profiles in single-stage fixed-bed reactors for CO_2-methanation. Chem Eng Sci. 2015;132:59-71.

[15] Xu J, Froment GF. Methane steam reforming, methanation and water-gas shift: I. Intrinsic kinetics. AIChE Journal. 1989;35:88-96.

[16] Gruber M, Weinbrecht P, Biffar L, Harth S, Trimis D, Brabandt J, et al. Power-to-Gas through thermal integration of high-temperature steam electrolysis and carbon dioxide methanation - Experimental results. Fuel Processing Technology. 2018;181:61-74.

[17] Lefebvre J, Bajohr S, Kolb T. Modeling of the transient behavior of a slurry bubble column reactor for CO_2 methanation, and comparison with a tube bundle reactor. Renewable Energy. 2020;151:118-36.

[18] Martin H, Nilles M. Radiale Wärmeleitung in durchströmten Schüttungsrohren. Chemie Ingenieur Technik. 1993;65:1468-77.

[19] Basu S, Khan AL, Cano-Odena A, Liu C, Vankelecom IFJ. Membrane-based technologies for biogas separations. Chemical Society Reviews. 2010;39:750-68.

[20] Gnielinski V. On heat transfer in tubes. Int J Heat Mass Tran. 2013;63:134-40.

[21] Shah MM. A general correlation for heat transfer during film condensation inside pipes. Int J Heat Mass Tran. 1979;22:547-56.

[22] Liu Z, Winterton RHS. A general correlation for saturated and subcooled flow boiling in tubes and annuli, based on a nucleate pool boiling equation. Int J Heat Mass Tran. 1991;34:2759-66.